Volume 3
Number 6
November 2025
Pages 1395-1650

RSC Applied Polymers

rsc.li/RSCApplPolym

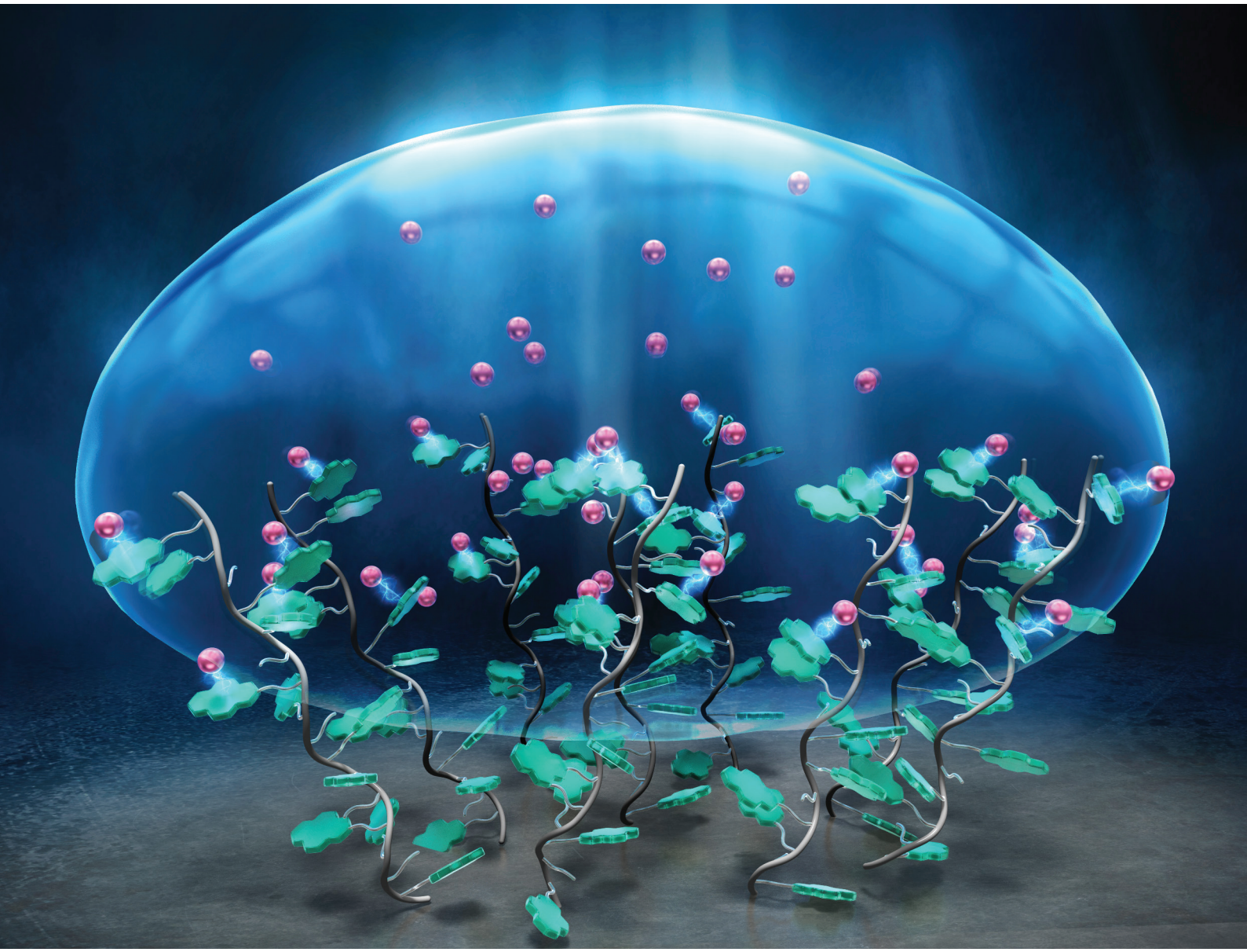

ISSN 2755-371X

ROYAL SOCIETY OF CHEMISTRY

PAPER
Masaaki Akamatsu, Hideki Sakai *et al.*
Solute-induced wettability control at naphthalenediimide polymer brushes *via* anion–π interactions

RSC Applied Polymers

PAPER

View Article Online
View Journal | View Issue

Cite this: *RSC Appl. Polym.*, 2025, **3**, 1452

Solute-induced wettability control at naphthalenediimide polymer brushes *via* anion–π interactions

Masaaki Akamatsu, *[a,b,c,d] Haduki Nakahara,[a] Ayumi Kimura,[a] Kyosuke Arakawa,[a] Shinsuke Ifuku,[c,d] Kenichi Sakai[a,b] and Hideki Sakai*[a,b]

Wettability at solid/liquid interfaces is a critical property that influences material functions such as sensing, mass transport, interfacial reactions, and adhesion. While selective wettability toward specific substances is desirable, established methods to achieve this remain limited. Noncovalent interactions, especially those driving molecular recognition and self-assembly, are essential for biological functions and functional molecular systems. However, their role in controlling the interfacial wettability has not been fully explored. In this study, we aimed to control the water wettability using anion–π interactions between anions and electron-deficient aromatic rings. To enhance these interactions, polymer brushes bearing naphthalenediimide (NDI) units serving as anion receptors have been fabricated on solid substrates. Quartz crystal microbalance with dissipation (QCM-D) measurements revealed strong and selective adsorption of nitrate ions (NO_3^-). Force curve analysis was used to further quantify the anion–π interactions at the interface. When aqueous solutions containing various anions were applied to the NDI-modified surfaces, a decrease in the contact angle was observed compared to that of pure water, indicating enhanced wettability. Notably, the NO_3^- solutions led to a significant reduction in the contact angle, which is consistent with the adsorption data. These findings demonstrate successful modulation of wettability through molecular recognition, specifically *via* anion–π interactions. This approach offers a promising strategy for developing selective wetting interfaces. Future work may involve integrating electrowetting mechanisms to expand their applications in sensors, controlled substance transport, and separation technologies.

Received 1st September 2025,
Accepted 11th October 2025

DOI: 10.1039/d5lp00275c

rsc.li/rscapplpolym

Introduction

Non-covalent interactions (*e.g.*, hydrogen bonds and van der Waals forces) drive the formation of a variety of self-assembled structures, including micelles, vesicles, liquid crystals, supramolecular polymers, and higher-order structures created by proteins and DNA or RNA.[1–5] These structures are essential for biological functions. Additionally, precise molecular recognition associated with these inter- and intra-molecular interactions plays a significant role in selective chemical reactions and mass transport in biological membranes.[6,7] These interactions can also influence the properties of the liquid/solid interfaces, such as wetting, friction, adhesion, and particulate dispersion.

Recently, considerable attention has been devoted to the wetting phenomena of solids adapting to the contacting liquid.[8] This adaptive wetting originates from the affinity based on molecular interactions between the functional groups near the solid interface and the liquid. Conversely, selective wetting is expected to occur by designing this intermolecular interaction. This enables the construction of functional interfaces for sensing, mass transport, separation of water/oil components, efficiency of interfacial reactions, adhesion, cell screening, and the reduction of friction.[9–11]

Thus far, selective wetting has been achieved through chemical processes involving silane coupling agents or microfabrication technologies.[10,12] Solid interfaces that provide novel selective wettability for compounds with significantly different properties (*e.g.*, polarity) have been reported. However, selectivity for similar molecules or atoms has not yet

[a]*Department of Pure and Applied Chemistry, Faculty of Science and Technology, Tokyo University of Science, 2641 Yamazaki, Noda, Chiba 278-8510, Japan. E-mail: hisakai@rs.tus.ac.jp*
[b]*Research Institute for Science and Technology, Tokyo University of Science, 2641 Yamazaki, Noda, Chiba 278-8510, Japan*
[c]*Department of Chemistry and Biotechnology, Faculty of Engineering, Tottori University, 4-101 Koyama-Minami, Tottori, Tottori 680-8550, Japan*
[d]*Research Institute for Sustainable Humanosphere, Kyoto University, Gokasho, Uji, Kyoto 611-0011, Japan. E-mail: akamatsu.masaaki.6t@kyoto-u.ac.jp*

been fully achieved. Takahara and Huck have reported tuning the wettability of water or oil using ionic or zwitterionic polymer brushes by taking advantage of the contraction or expansion of the polymer due to the formation of ion pairs during ion additions.[13–16] Shundo and Tanaka succeeded in recognizing the *R* and *S* isomers of chiral liquid molecules using a cast film of chiral polymers.[17] However, the design of selective wetting for desired compounds or their solutions remains challenging.

Recently, as a new anion recognition mechanism, anion–π interactions between anions and aromatic rings have attracted much attention.[18–22] By introducing a strong electron-withdrawing group into an aromatic ring, its quadrupole moment (Q_{zz}) is inverted and an attractive interaction occurs, acting as an anion receptor. The introduction of functional groups, such as naphthalenediimide (NDI), is a typical skeleton that can be functionalized by introducing functional groups.[23] The anion–π interaction plays an important role in the formation of higher-order structures of proteins and in enzymatic reactions.[24,25] This has been applied to anion sensors,[26] artificial ion channels,[27] and homogeneous organocatalysts,[28,29] as well as for the control of molecular assembly[20] and catalytic activity by electric fields[30,31] on electrode surfaces. Our group reported reversible adsorption and desorption of anions upon two-dimensional mechanical stimulation using a monolayer of amphiphilic NDI at the air/water interface.[32,33] The anion adsorption capacity was found to be affected not only by the functional group but also by the association state and environment. Furthermore, we reported on mechanoelectrical transduction, which evokes a signaling mechanism in living organisms *via* anion adsorption ability.[33] This suggests that the interface is an effective platform for amplifying the anion recognition ability to macroscale properties.

On the other hand, Zeng *et al.* revealed that this anion–π interaction also contributes to the bioadhesion mechanism, based on the evaluation of the solid film of polycatechol and the water interface by surface force measurements.[34–36] Our group quantitatively evaluated the adsorption properties of anions at the solid/water interface by forming monolayers of NDI derivatives (Fig. 1(b), **monoNDI@silica**) using quartz crystal microbalance with dissipation (QCM-D) measurements.[37] It was found that flat nitrate ions (NO_3^-) exhibited excellent adsorption at the interfacial film. Furthermore, force curve measurements by atomic force microscopy (AFM) revealed that the single force of the anion–π interaction between the NDI unit as a receptor and the negative charge is ~40 pN. However, the control of water wettability by anion addition is trivial. This may be due to the low number of functional groups present at the interface in the monolayer and the weak total force of anion–π interactions at the interface.

In this study, NDI-modified polymer brushes were synthesized to increase the number of anion adsorption sites and amplify the anion–π interactions at the solid/water interface (Fig. 1). This was aimed at controlling wettability by increasing the affinity between the solid interface and water, driven by the adsorption of anions on the NDI moieties (Fig. 1(c)). A

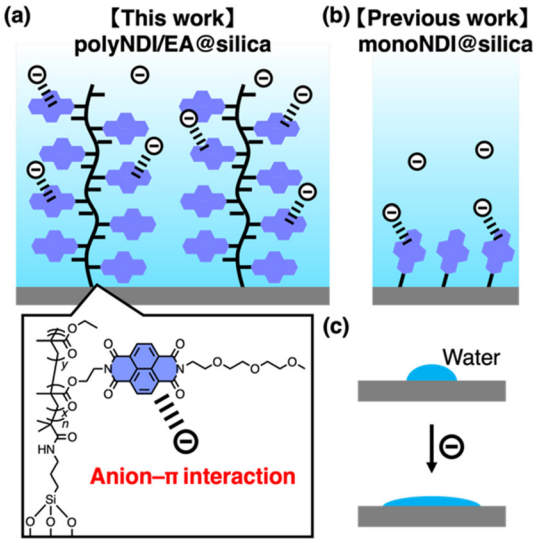

Fig. 1 Anion–π interaction at water/solid interfaces using NDI-modified polymer brush (**polyNDI/EA@silica**) and monolayer (**monoNDI@silica**) (a and b). Enhancement of water wettability of the solid surface with anions in aqueous solutions (c).

copolymer brush was synthesized from monomers of NDI-modified (NDI) and ethyl methacrylates (EA) (Fig. 1(a), **polyNDI/EA@silica**). The anion adsorption capacities of the synthesized NDI-modified copolymer brushes were evaluated by QCM-D measurements. In addition, anion–π interactions at the solid/water interface were quantified using force-curve measurements. Furthermore, the contact angles of "aqueous" solutions containing different anion species were measured, and the control of water wettability by anion addition is discussed from the viewpoint of interfacial energy. By achieving water wettability control associated with anion adsorption, we expect to be able to construct selective wetting interfaces by designing receptor sites in the future.

Results and discussion

A methacrylate copolymer brush (**polyNDI/EA@silica**) composed of NDI units bearing tetraethylene glycol monomethyl (TEG) groups as the hydrophilic moieties and ethyl units was designed (Fig. 1(a)). The monomer containing the NDI group was synthesized in five steps, and the polymer brush was prepared on a silica substrate *via* surface-initiated atom transfer radical polymerization (SI-ATRP),[38] using a copolymerization of the NDI monomer with ethyl methacrylate at a feed molar ratio of 1 : 1 (Scheme S1). Spectroscopic ellipsometry confirmed the formation of an organic film with a thickness of ~8 nm in the dry state, and infrared (IR) spectroscopy using the ATR mode revealed peaks attributed to the C=O stretching vibrations of ester and imide groups (1725 and 1640 cm^{-1}, respectively), as well as peaks derived from the C–C stretching vibrations of aromatic rings (1560 cm^{-1}), reflecting the molecular structure of the polymer brush (Fig. S3). These results

collectively confirm the successful formation of the polymer brushes.

The amount of anions adsorbed on the substrate was evaluated using the QCM-D technique. A decrease in the frequency shift (ΔF_n) was observed in flowing aqueous solutions of tetrabutylammonium salts of various anions (Fig. S4), indicating ion adsorption, similar to the results previously reported for a monolayer system (**monoNDI@silica**).[37] However, in contrast to the previous monolayer system, the dissipation shift (ΔD_n), which reflects the viscoelastic properties of the film, exhibited an overtone dependence (Fig. S5). The penetration depth of oscillation on the vertical direction of the film depends on the overtone number. If the molecular film is sufficiently thick, overtone number affects ΔF_n and ΔD_n.[39] This behavior indicated the formation of a viscosity-dominant "soft" film consisting of polymer brushes. Nevertheless, this also implies that the commonly used Sauerbrey equation is not applicable to calculating adsorption amounts in such cases. Therefore, based on the viscoelastic model,[39] the adsorption amounts were calculated using the ΔF_n and ΔD_n values at different overtone numbers.

Theoretically, anion–π interactions are stronger for anions with higher charge densities, that is, those with larger hydration energies (ΔG_{hyd}). ΔG_{hyd} represents the stabilization energy associated with complete hydration of a bare ion, and it reflects the charge density of the ion. Fig. 2 shows the adsorption amount plotted against the hydration energy of each anion. Similar to the previously reported monolayer system,[37] halide ions, such as Cl^-, Br^-, and I^-, as well as sulfate ions (SO_4^{2-}), followed this trend. However, nitrate ions (NO_3^-) exhibited unusually strong adsorption. This is likely due to the additional π–π stacking interaction between the π-conjugated system of NO_3^- and NDI units.

Compared with the monolayer system, the polymer brush exhibited an overall ~6-fold increase in the adsorption amount. This enhancement was attributed to the increased number of adsorption sites introduced by the polymer brush structure. Interestingly, for NO_3^-, a particularly large ~12-fold increase in adsorption was observed. This may be explained by the formation of spatial environments within the polymer brush that are well suited to the size and shape of the planar structure of NO_3^-, thereby facilitating stronger interactions with the NDI sites.

In contrast, the homopolymer brush composed solely of NDI units (**polyNDI@silica**) showed almost no adsorption of anions. Therefore, the aggregation state of the NDI moieties within the film was evaluated based on the absorbance ratio of I_{0-0} to I_{0-1} (I_{0-0}/I_{0-1}) derived from the NDI units using UV/vis absorption spectroscopy (Fig. S6). For **polyNDI@silica**, the characteristic absorption bands of the NDI moiety were observed at 358 nm and 378 nm, originating from the 0–0 and 0–1 vibronic transitions, respectively.[26] Compared to **monoNDI@silica** and the monomer (MAA-NDI-TEG) in chloroform solution, **polyNDI@silica** exhibited a markedly decreased I_{0-0}/I_{0-1} ratio, indicating that the NDI units were in a strongly aggregated state and that the adsorption sites on the NDI moieties were lost. These findings suggest that copolymerization with ethyl acrylate effectively secured sufficient adsorption sites, which are essential for anion adsorption.

Next, to directly evaluate the anion–π interactions at the solid/water interface, force curve measurements were conducted using AFM. Fig. 3(a) shows the force curves with the force on the vertical axis and the apparent distance on the horizontal axis. In water, **polyNDI/EA@silica** exhibited an attractive force, similar to that previously reported **for monoNDI@silica**.[37] This attraction is considered to arise from the anion–π interaction between the negatively charged cantilever (silicon nitride) in water and NDI moieties on the polymer brush. In contrast, for the poly(ethyl acrylate) brush (**polyEA@silica**) without NDI moieties, only repulsive forces were observed (Fig. 3(a)), indicating that the attractive force observed with **polyNDI/EA@silica** was a specific interaction derived from the NDI units. Furthermore, histogram analysis of the measured forces revealed that the average attractive force was −0.92 nN, approximately 13 times greater than that observed in monolayer systems (Fig. 3(b)). In addition, the onset distance at which the attractive force was detected shifted to approximately 6 nm, indicating both enhancement of the interaction and film thickening due to brush formation.

In addition, the single-molecule force of the anion–π interaction between the NDI moiety on the substrate and the negative charge on the cantilever was calculated through autocorrelation analysis[40] of the attractive forces observed in pure water (Fig. 3(c)). The periodicity in the autocorrelation function indicated that the single-molecule force derived from the anion–π interaction for **polyNDI/EA@silica** was approximately 40–50 pN. This value is close to the result obtained for **monoNDI@silica** (~40 pN),[37] suggesting that the observed interaction originates from a one-to-one interaction between a single negative charge on the cantilever and a single NDI unit on the substrate, regardless of whether it occurs in a monolayer or polymer brush. In other words, the increase in the total anion–π interaction strength upon brush formation was

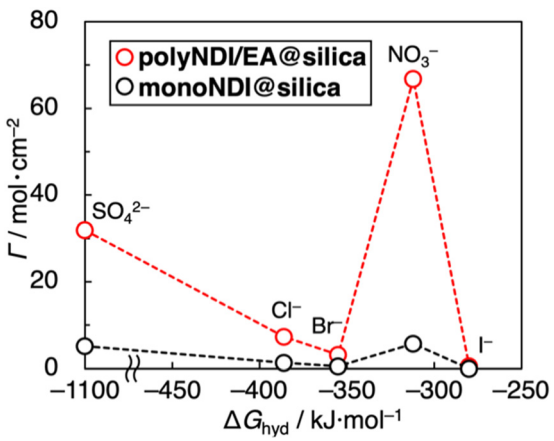

Fig. 2 Plots of the adsorption amount of the anions (Γ) of **polyNDI/EA@silica** and **monoNDI@silica** *vs.* the hydration energy of the anion species (ΔG_{hyd}).

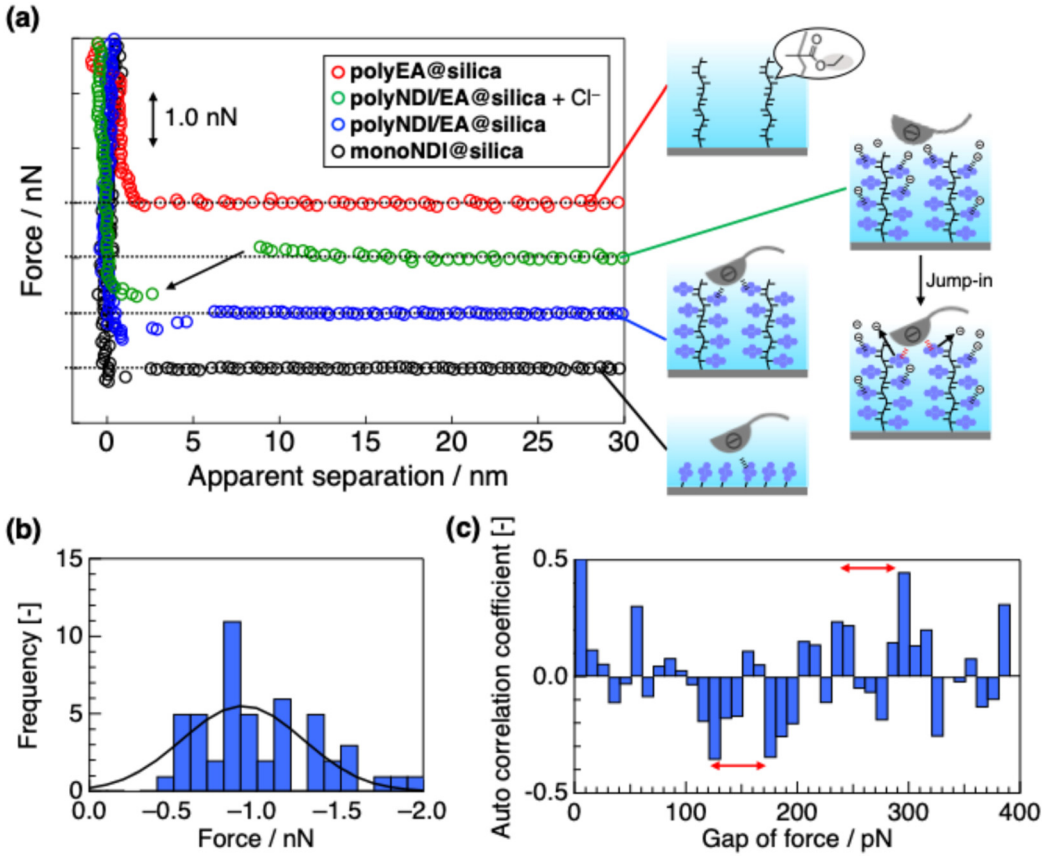

Fig. 3 (a) Approaching force curves of **polyEA@silica** in pure water, **polyNDI/EA@silica** in pure water or aqueous 10 mM TBACl solution, and **monoNDI @silica** in pure water (from top to bottom). The *Z*-scale interval was 1.0 nN. (b) Histogram of the observed attractive force on the NDI-modified polymer brush in pure water in pure water (n = 100) and (c) its autocorrelation coefficient.

supported by the increased number of NDI moieties. In contrast, the slight enhancement of the single-molecule force on **polyNDI/EA@silica** compared to **monoNDI@silica** is derived from the delocalization of electrons through the inter- or intramolecular π stacks of the NDI units in the polymer brush film.[41]

Furthermore, upon the addition of 10 mM TBACl to water, a repulsive force was observed, followed by jump-in behavior (Fig. 3(a)). This repulsion is considered to result from the electrostatic repulsion between the anions adsorbed on the substrate and the negatively charged cantilever. As mechanical compression proceeds, Cl^- ions are expelled from the film, leading to the emergence of an attractive force, observed as a jump-in behavior.

Next, the attractive and repulsive forces observed upon the addition of various anions were analyzed as histograms (Fig. S7). The main components are summarized in Fig. 4. Before anion addition, only attractive forces were observed; however, upon the introduction of anions, a shift toward the repulsive force regions was detected. This transition to repulsion is particularly pronounced for anions with higher adsorption affinities. These results further support the presence of anion–π interactions between the **polyNDI/EA@silica** and the negatively charged cantilever.

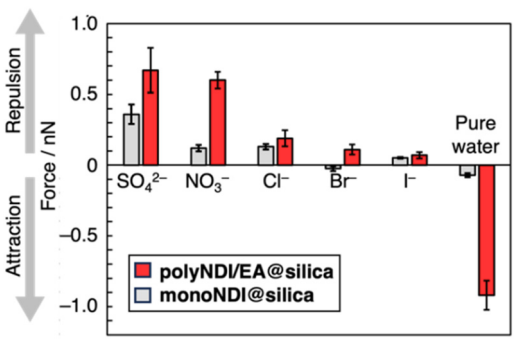

Fig. 4 Force detected on **polyNDI/EA@silica** and **monoNDI@silica** using force curve measurements in pure water or aqueous solutions of TBA_2SO_4, $TBANO_3$, TBACl, TBABr, or TBAI.

In contrast, in the homopolymer brush (**polyNDI@silica**), the increase in the repulsive forces upon anion addition was not significant (Fig. S8), which is likely due to the low anion adsorption. Moreover, the magnitude of the repulsive forces was greater than that observed for **monoNDI@silica**, clearly indicating that polymer brush formation enhances anion adsorption and alters the interaction accordingly.

With the formation of a polymer brush, enhancement of the anion–π interaction at the water/solid interface was confirmed. Next, we investigated the control of wettability by water driven by anion interactions. Fig. 5(a) shows the contact angles measured when 10 mM aqueous sodium salt solutions of various anions were dropped onto the NDI-modified substrate. In this characterization, we chose sodium salts instead of tetrabutylammonium salts, which are used for QCM-D and force curve measurements, because of the versatility of the salts for potential applications. Moreover, the relative hydrophobicity of the tetrabutylammonium cation may inhibit the enhancement of water wettability derived from anions.

The **polyNDI/EA@silica** surface exhibits a contact angle of 61.4° with water. In contrast, a decrease in the contact angle was observed for the anion-containing aqueous solutions, indicating enhanced wettability due to the presence of anions. Notably, in the case of NO_3^-, a maximum reduction of 29° in the contact angle was observed. Compared to previous results for monolayer systems, where the maximum change was approximately 7° for NO_3^- solutions, polymer brush formation enabled a dramatic anion-induced change in the contact angle.

The change in contact angle caused by the addition of solute anions is believed to result from the adsorption of anions onto the NDI moieties on the modified substrate after the aqueous solution comes into contact with the surface. This adsorption enhances the affinity of the substrate for water, owing to the charge of the anions and their associated hydration water. To confirm that anion adsorption served as the driving force, the contact angles were plotted against the adsorption amounts of each anion, as shown in Fig. 5(b). A decrease in the contact angle was observed with increasing adsorption amount.

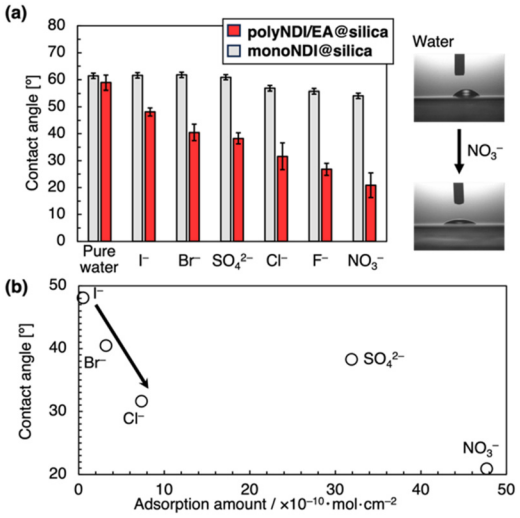

Fig. 5 (a) Contact angles of **polyNDI/EA@silica** and **monoNDI@silica** for pure water and aqueous solutions of Na_2SO_4, $NaNO_3$, NaF, NaCl, NaBr, and NaI, and photographs of pure water and aqueous solution of $NaNO_3$. The concentration of the sodium salts was fixed at 10 mM. (b) Contact angle *vs.* adsorption amount of anions.

In particular, for halide anions (I^-, Br^-, and Cl^-), the contact angle linearity decreased with increasing adsorption amount. However, NO_3^-, which exhibited the largest change in contact angle, deviated from this linear trend. As shown in Fig. 2, this is likely because NO_3^- has a hydration energy comparable to that of I^-, meaning its hydration ability is low. This result further supports the idea that partially hydrated water molecules surrounding the interfacial anions contribute to affinity toward the bulk liquid (water). Therefore, to maximize wettability changes, the intrinsic properties of the anions must also be considered. Additionally, SO_4^{2-} showed a contact angle change similar to that of Br^-, despite its adsorption amount being only approximately one-tenth. This deviation from the trend was likely due to the dehydration effect associated with SO_4^{2-}.

As described above, we observed changes in wettability driven by anion adsorption, which, in turn, was driven by anion–π interactions with the polymer brush substrate. To quantify the enhanced affinity between the anion-containing aqueous solutions and the polymer brush surface, the interfacial free energy (γ_{sl}) was calculated using the surface tension of the aqueous solution (γ_{lg}) and the surface free energy of the substrate (γ_{sg}) based on Young's equation (eqn (1)). The results are listed in Fig. 6.

$$\gamma_{sg} = \gamma_{sl} + \gamma_{lg} \cos\theta \quad (1)$$

Consequently, a decrease in the interfacial free energy upon anion addition was observed for the polymer brush substrate (Fig. 6). This confirms that anion addition plays a role in stabilizing the substrate–water interface by enhancing the affinity between the two phases. In contrast, while some interfacial stabilization was also observed for the monolayer substrate upon anion addition, the extent of the change was only approximately one-third of that seen with the polymer brush substrate, consistent with the abovementioned results.

With respect to the contact angle, although the addition of salts contributes to changes in surface tension, such variations are limited to only a few mN m^{-1}. By contrast, the free energy

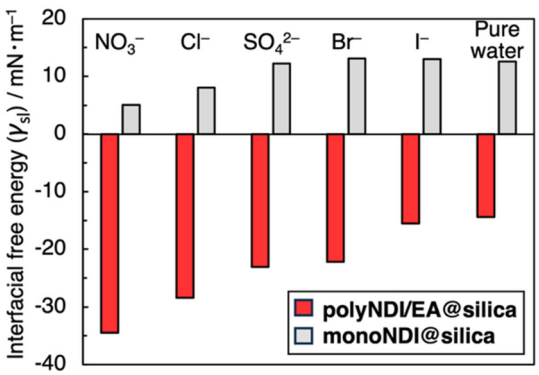

Fig. 6 Interfacial free energies of **polyNDI/EA@silica** and **monoNDI@silica** for pure water and aqueous solutions of Na_2SO_4, $NaNO_3$, NaCl, NaBr, and NaI according to contact angle measurements.

of the solid/liquid interface (γ_{sl}) calculated in the present study exhibits a pronounced change on the order of several tens of mN m^{-1}. This indicates that the interfacial energy modulation arising from the specific adsorption behavior of anionic species at the interface constitutes the predominant factor governing the observed variation in contact angle. Furthermore, a good linear relationship was found between the contact angle and interfacial free energy (Fig. S9), indicating that the contact angle change strongly depends on the interfacial stabilization driven by anion adsorption *via* anion–π interactions.

These findings demonstrate that wettability can be effectively controlled through interfacial energy stabilization driven by anion adsorption. To the best of our knowledge, this is the first example in which the selectivity of molecular recognition has been directly linked to interfacial properties.

Conclusions

The anion adsorption enhancement and wettability control of water were investigated using naphthalenediimide (NDI)-modified polymer brushes. Compared to previously reported monolayer substrates, the NDI and ethyl acrylate copolymer brush substrates exhibited a significant increase in both the amount of anion adsorption and the attractive force derived from anion–π interactions. Autocorrelation analysis revealed that the 1 : 1 intermolecular force between an NDI unit and a negative charge was approximately 40–50 pN, similar to previous systems, confirming that the amplified attractive force was due to an increased number of NDI units.

Furthermore, the water contact angle on the NDI/EA copolymer brush substrate decreased with the addition of anions. This enhancement in wettability was dependent on both the amount and type of anions adsorbed. The observed change originated from a reduction in the interfacial free energy between the substrate and water, which was attributed to the increased surface charge resulting from anion adsorption onto the NDI units and associated hydration water. This represents the first example of wettability control at a solid/liquid interface based on molecular recognition.

By utilizing the physical properties of solid/liquid interfaces, this approach holds promise for sensing applications, where outputs such as wettability and particle dispersibility can be leveraged. Through the appropriate design of substituents on the NDI framework and polymer structure, selective wettability control tailored to specific purposes is expected to become feasible in the future.

Recent studies have reported the use of electrowetting for sensing, material separation, and liquid transport.[42,43] Matile and Akamatsu also reported the electric field control of anion–π interactions.[30,31] By further developing the selective wetting behavior induced by solute anions identified in this study and combining it with electrowetting techniques, it may be possible to achieve spatiotemporal control of wettability. This can pave the way for advanced sensing technologies, selective material separation, and precise mass transport.

Author contributions

H. N. and A. K. conducted synthesis and characterization of polymer brushes. S. I. measured the molecular weight of the polymers. K. A. helped data interpretation of the spectroscopic measurements. M. A. and H. S. handled conceptualization, writing, and editing of the manuscript.

Conflicts of interest

There are no conflicts to declare.

Data availability

Supplementary information (SI): experimental details and data from the NMR, MS, UV/vis, IR, and QCM-D. See DOI: https://doi.org/10.1039/d5lp00275c.

Acknowledgements

This work was supported by the Foundation, Oil & Fat Industry Kaikan, Foundation for the Promotion of Ion Engineering, Iketani Science and Technology Foundation, and JSPS KAKENHI Grant Number JP25K08751.

References

1 H. Schneider, *J. Phys. Org. Chem.*, 2022, **35**, e4340.
2 J. B. Engberts and J. Kevelam, *Curr. Opin. Colloid Interface Sci.*, 1996, **1**, 779–789.
3 C. Rest, R. Kandanelli and G. Fernández, *Chem. Soc. Rev.*, 2015, **44**, 2543–2572.
4 H. He, W. Tan, J. Guo, M. Yi, A. N. Shy and B. Xu, *Chem. Rev.*, 2020, **120**, 9994–10078.
5 K. Liu, Y. Kang, Z. Wang and X. Zhang, *Adv. Mater.*, 2013, **25**, 5530–5548.
6 J. J. García, L. López-Pingarrón, P. Almeida-Souza, A. Tres, P. Escudero, F. A. García-Gil, D. Tan, R. J. Reiter, J. M. Ramírez and M. Bernal-Pérez, *J. Pineal Res.*, 2014, **56**, 225–237.
7 G. L. Nicolson, *Biochim. Biophys. Acta, Biomembr.*, 2014, **1838**, 1451–1466.
8 H.-J. Butt, R. Berger, W. Steffen, D. Vollmer and S. A. L. Weber, *Langmuir*, 2018, **34**, 11292–11304.
9 D. Tian, Y. Song and L. Jiang, *Chem. Soc. Rev.*, 2013, **42**, 5184.
10 P. Gupta and B. Kandasubramanian, *ACS Appl. Mater. Interfaces*, 2017, **9**, 19102–19113.
11 X. Bai, Z. Yuan, C. Lu, H. Zhan, W. Ge, W. Li and Y. Liu, *Nanoscale*, 2023, **15**, 5139–5157.
12 C. G. J. Prakash and J.-W. Lee, *J. Mater. Sci.*, 2023, **58**, 6775–6783.

13 Y. Higaki, Y. Inutsuka, T. Sakamaki, Y. Terayama, A. Takenaka, K. Higaki, N. L. Yamada, T. Moriwaki, Y. Ikemoto and A. Takahara, *Langmuir*, 2017, **33**, 8404–8412.
14 Y. Higaki, M. Kobayashi and A. Takahara, *Langmuir*, 2020, **36**, 9015–9024.
15 Y. Higaki, R. Furusawa, T. Otsu and N. L. Yamada, *Langmuir*, 2022, **38**, 9278–9284.
16 O. Azzaroni, S. Moya, T. Farhan, A. A. Brown and W. T. S. Huck, *Macromolecules*, 2005, **38**, 10192–10199.
17 A. Shundo, K. Hori, T. Ikeda, N. Kimizuka and K. Tanaka, *J. Am. Chem. Soc.*, 2013, **135**, 10282–10285.
18 I. A. Rather, S. A. Wagay and R. Ali, *Coord. Chem. Rev.*, 2020, **415**, 213327.
19 M. Giese, M. Albrecht and K. Rissanen, *Chem. Commun.*, 2016, **52**, 1778–1795.
20 D.-X. Wang and M.-X. Wang, *Acc. Chem. Res.*, 2020, **53**, 1364–1380.
21 Y. Zhao, Y. Cotelle, L. Liu, J. López-Andarias, A.-B. Bornhof, M. Akamatsu, N. Sakai and S. Matile, *Acc. Chem. Res.*, 2018, **51**, 2255–2263.
22 Z. Liu, Z. Chen and X. Xu, *CCS Chem.*, 2021, **3**, 904–915.
23 N. Sakai, J. Mareda, E. Vauthey and S. Matile, *Chem. Commun.*, 2010, **46**, 4225.
24 X. Lucas, A. Bauzá, A. Frontera and D. Quiñonero, *Chem. Sci.*, 2016, **7**, 1038–1050.
25 C. Estarellas, A. Frontera, D. Quiñonero and P. M. Deyà, *Angew. Chem., Int. Ed.*, 2011, **50**, 415–418.
26 S. Guha and S. Saha, *J. Am. Chem. Soc.*, 2010, **132**, 17674–17677.
27 R. E. Dawson, A. Hennig, D. P. Weimann, D. Emery, V. Ravikumar, J. Montenegro, T. Takeuchi, S. Gabutti, M. Mayor, J. Mareda, C. A. Schalley and S. Matile, *Nat. Chem.*, 2010, **2**, 533–538.
28 Y. Zhao, S. Benz, N. Sakai and S. Matile, *Chem. Sci.*, 2015, **6**, 6219–6223.
29 Y. Zhao, Y. Cotelle, A.-J. Avestro, N. Sakai and S. Matile, *J. Am. Chem. Soc.*, 2015, **137**, 11582–11585.
30 M. Akamatsu, N. Sakai and S. Matile, *J. Am. Chem. Soc.*, 2017, **139**, 6558–6561.
31 M. Á. Gutiérrez López, A. Marsalek, N. Sakai and S. Matile, *Chem. Sci.*, 2025, **16**, 11264–11269.
32 M. Akamatsu, K. Yamanaga, K. Tanaka, Y. Kanehara, M. Sumita, K. Sakai and H. Sakai, *Langmuir*, 2023, **39**, 5833–5839.
33 M. Ishii, Y. Nakai, S. Kaneko, K. Tanaka, Y. Yamashita, K. Sakai, H. Sakai, K. Ariga and M. Akamatsu, *Langmuir*, 2024, **40**, 27040–27048.
34 J. Zhang, L. Xiang, B. Yan and H. Zeng, *J. Am. Chem. Soc.*, 2020, **142**, 1710–1714.
35 B. Yan, Z. Lv, S. Chen, L. Xiang, L. Gong, J. Xiang, H. Fan and H. Zeng, *J. Colloid Interface Sci.*, 2022, **615**, 778–785.
36 M. Wu, L. Han, B. Yan and H. Zeng, *Supramol. Mater.*, 2023, **2**, 100045.
37 M. Akamatsu, A. Kimura, K. Yamanaga, K. Sakai and H. Sakai, *Chem. Commun.*, 2021, **57**, 4650–4653.
38 K. Ślusarczyk, M. Flejszar and P. Chmielarz, *Polymer*, 2021, **233**, 124212.
39 A. D. Easley, T. Ma, C. I. Eneh, J. Yun, R. M. Thakur and J. L. Lutkenhaus, *J. Polym. Sci.*, 2022, **60**, 1090–1107.
40 H. Schönherr, M. W. J. Beulen, J. Bügler, J. Huskens, F. C. J. M. Van Veggel, D. N. Reinhoudt and G. J. Vancso, *J. Am. Chem. Soc.*, 2000, **122**, 4963–4967.
41 A.-B. Bornhof, A. Bauzá, A. Aster, M. Pupier, A. Frontera, E. Vauthey, N. Sakai and S. Matile, *J. Am. Chem. Soc.*, 2018, **140**, 4884–4892.
42 A. A. Papaderakis, A. Ejigu, J. Yang, A. Elgendy, B. Radha, A. Keerthi, A. Juel and R. A. W. Dryfe, *J. Am. Chem. Soc.*, 2023, **145**, 8007–8020.
43 P. Teng, D. Tian, H. Fu and S. Wang, *Mater. Chem. Front.*, 2020, **4**, 140–154.